Electronic Supplementary Material (ESI) for Nanoscale.
This journal is © The Royal Society of Chemistry 2020

Supplementary information

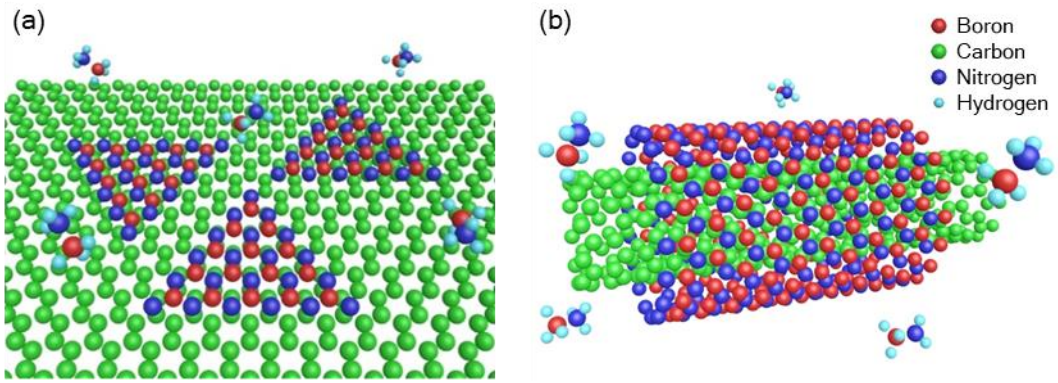

Figure S1. Schematic illustration of non-catalytic growth of h-BN on graphene-based materials in various dimensions. (a) two-dimensional (2D) growth of h-BN on graphene, and (b) one-dimensional (1D) growth of boron nitride nanotubes on single walled carbon nanotubes. Although curvature may affect the reaction for the growth of h-BN, such as, adsorption and desorption of the precursor onto single walled carbon nanotubes, the insight for 2D-growth can be useful for effective 1D-growth.

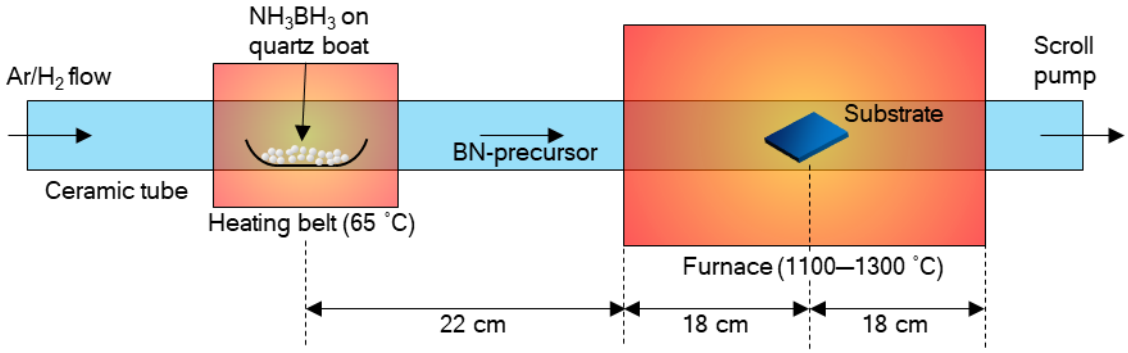

Figure S2. Schematic illustration of the CVD system. Our CVD system for h-BN growth was composed of a ceramic tube, a furnace, and a scroll pump. For h-BN growth, substrates and ammonia borane on a quartz boat were introduced into the ceramic tube. To supply a BN-precursor, ammonia borane was heated at 65 °C using a heating belt.

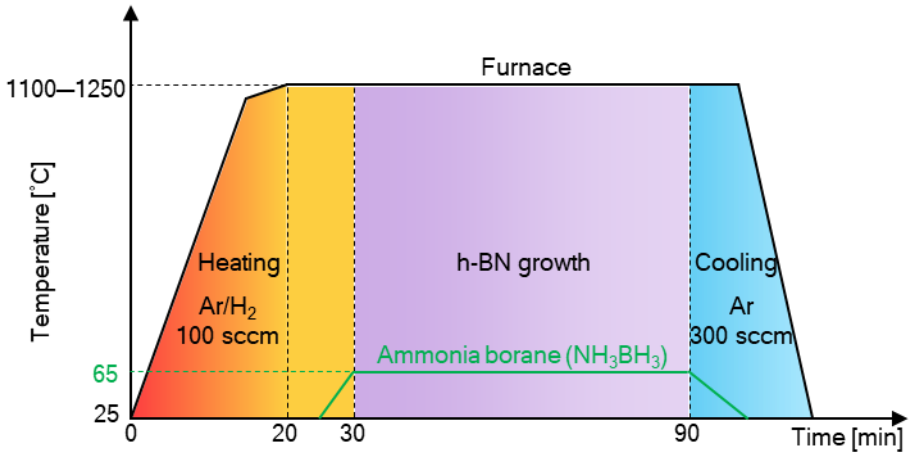

Figure S3. Schematic of a CVD growth process of h-BN on graphite. The furnace was heated up under an Ar/H_2 flow of 100 sccm. After the furnace reached the targeted growth temperature and was kept at this temperature for 10 min for stabilisation, h-BN growth was initiated by supplying ammonia borane as a precursor. A heating belt was used to heat ammonia borane, as shown in Fig. S2. The heating and cooling of ammonia borane took 3–5 min. After cooling of the ammonia borane, the furnace and the substrate inside the chamber were quickly cooled down to room temperature.

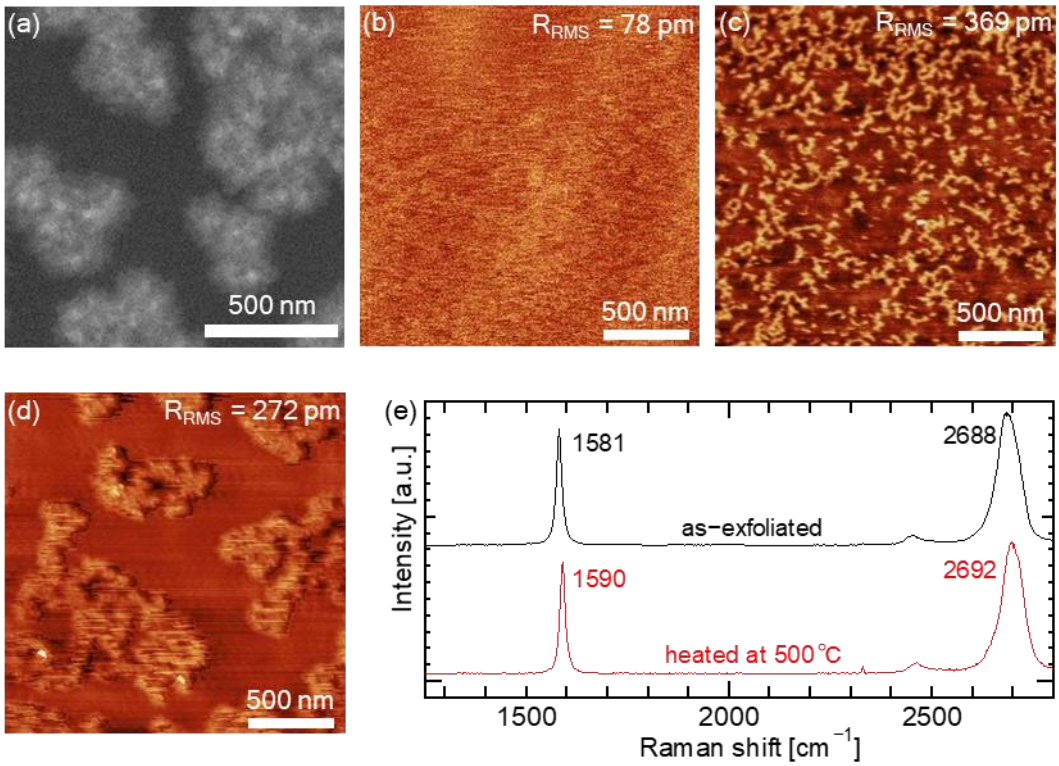

Figure S4. Pretreatment of graphite before h-BN growth. (a) SEM image of h-BN grown on graphite heated in air at 400 °C. BN-nucleation occurred so densely that individual domains cannot be seen. (b) AFM image of an as-exfoliated graphite surface. The surface was flat and without impurities just after exfoliation. (c) AFM image of a graphite surface after it was soaked in acetone. The graphite surface became rough. We supposed that tape residue was dispersed through acetone and deposited onto the graphite surface. (d) AFM image of the graphite surface annealed at 1100 °C in hydrogen after acetone treatment. The aggregated particle on the graphite surface is supposed to cause nucleation of h-BN with too high density. (e) Raman spectra taken from bilayer graphene on SiO_2. The black line represents the bilayer graphene and the red represents the bilayer graphene heated at 500 °C. Even for the bilayer graphene, which is more easily oxidised than bulk graphite, the increase in the D-band by 500 °C of heating was negligible.

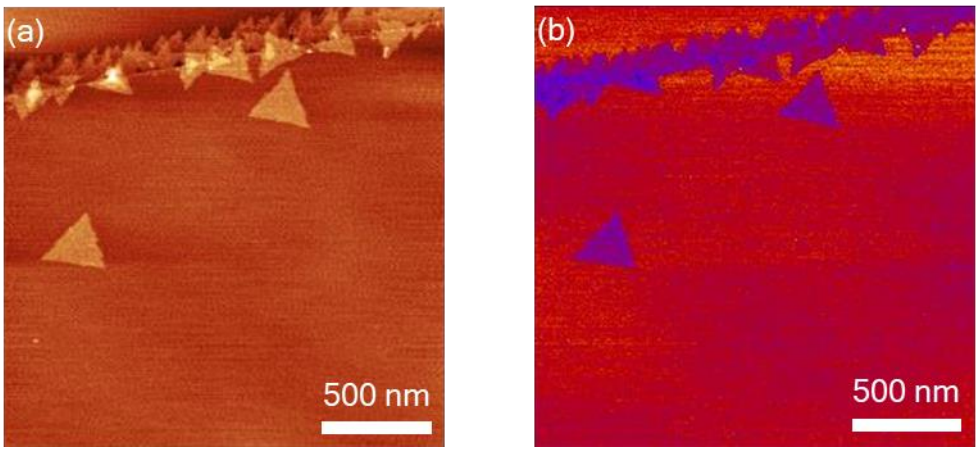

Figure S5. AFM shape and phase images. (a) AFM shape image of h-BN single-crystals and polycrystals grown along the step edge of graphite. (b) AFM phase image corresponding to (a). This reveals that AFM can distinguish bare h-BN from graphite according to the phase signal, which is affected by the interaction between probe tips and sample surfaces. Furthermore, the uniform phase signals from graphite and h-BN indicate almost no impurities on them.

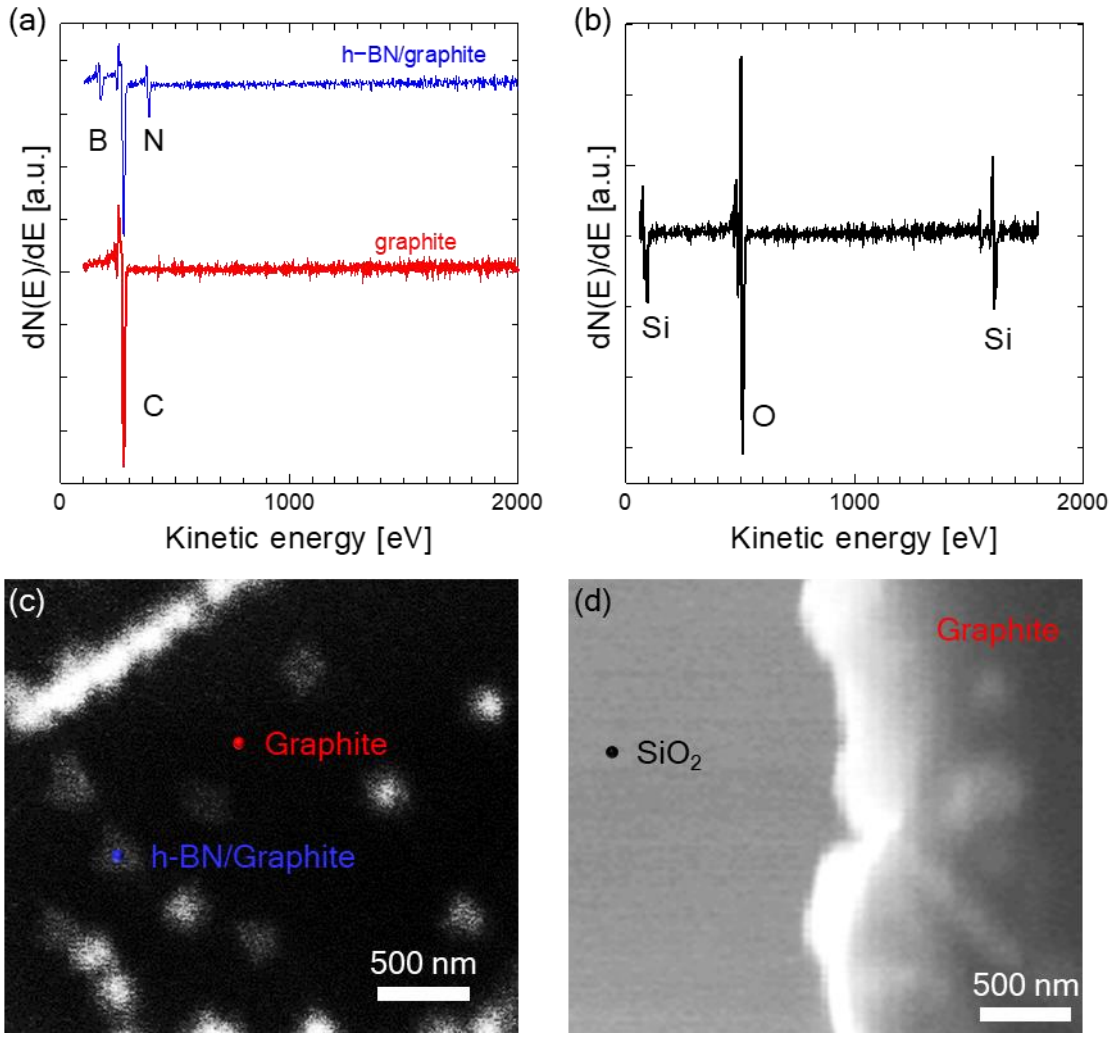

Figure S6. AES data from the sample after h-BN growth. (a) Wide range version of AES spectra shown in Fig. 1. (d). (b) AES spectrum taken from SiO_2 surface after h-BN growth. (c) SEM image of the graphite surface after h-BN growth taken by the AES facility. The spectra in (a) were taken from the blue and red dots. (d) SEM image of the edge of a graphite flake. The spectrum in (b) was taken from the black dot. The SEM images are relatively noisy because the current of the electron beam was reduced in order to prevent samples from charging up. Detection of only B, C, and N atoms on graphite surfaces confirmed impurity-free growth of h-BN on graphite. On the other hand, only O and Si atoms were detected on SiO_2 surfaces, indicating no h-BN growth on SiO_2.

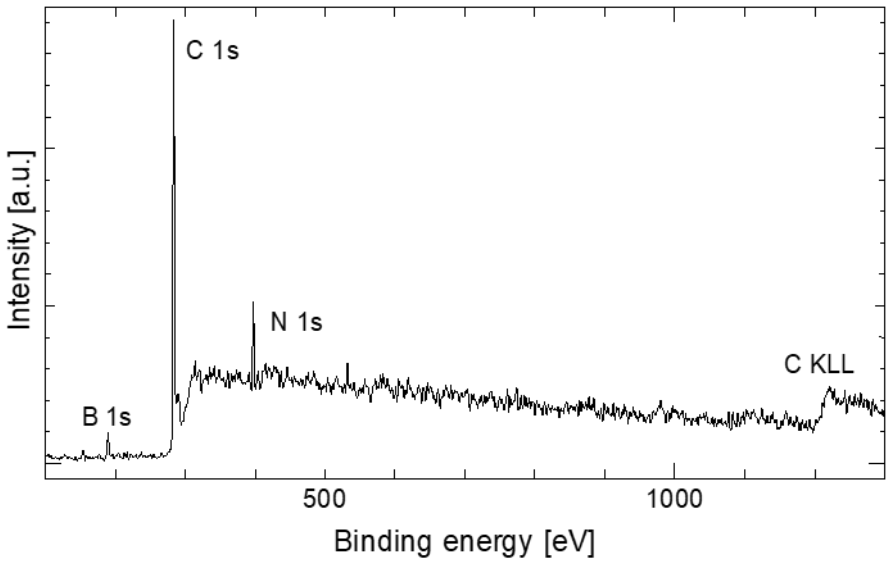

Figure S7. XPS spectrum taken from h-BN/graphite in a wide spectral region. B, N, and C signals can be observed. The signals of other atoms cannot be detected.

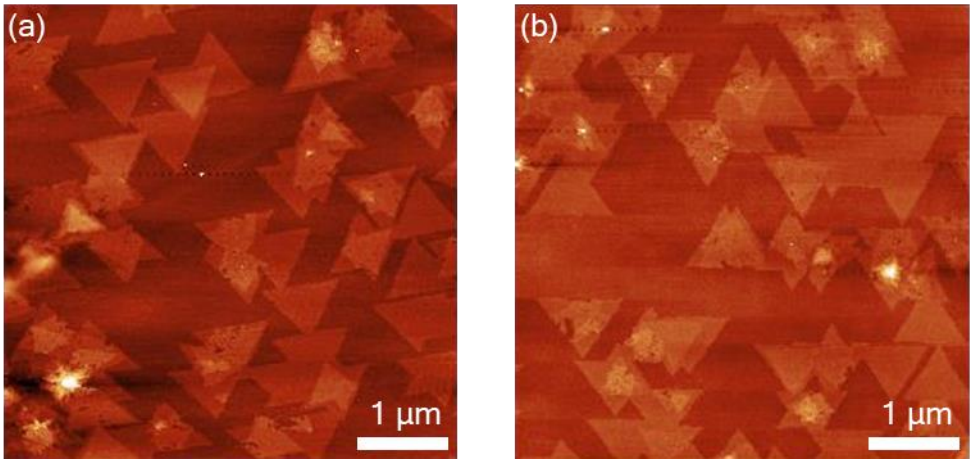

Figure S8. Additional AFM data of h-BN grown with the optimised conditions. (a, b) AFM images of other regions in the same sample as Fig. 6. Multiple triangular domains were uniformly grown to an edge length of ~1 μm even at different regions. Some h-BN single-crystals coalesced with adjacent domains to form polycrystals. Typically, the increase in the size of single-crystals was hindered by coalescence. To further increase the size of single-crystals, it is required to decrease nucleation density and thus prevent coalescence.